J MATER SCI **41** (2006) 1325–1333

In situ type study of hydrothermally prepared titanates and silicotitanates

A. CLEARFIELD*, A. TRIPATHI, D. MEDVEDEV
Department of Chemistry, Texas A&M University, College Station, TX, USA
E-mail: clearfield@mail.chem.tamu.edu

A.J. CELESTIAN, J.B. PARISE
State University of New York, Stony Brook, NY

One of the most vexing problems facing the nuclear industry and countries with nuclear weapons is the safe disposal of the generated nuclear waste. Huge quantities of nuclear waste arising from weapons manufacture are stored at the Hanford and Savannah River sites in the USA. The general method of remediation involves the removal of Cs-137, Sr-90 and actinides from a huge quantity of salts, principally $NaNO_3$, organics and complexing agents. It has been found that a sodium silicotitanate is able to remove Cs^+ selectively from the waste and certain sodium titanates remove Sr^{2+} and actinides. These compounds have been prepared by *ex-situ* hydrothermal methods. We have studied the *in situ* growth of these materials at the National Synchrotron Light Source, Brookhaven National Laboratory. In addition we will describe the mechanism of ion exchange in the titanosilicate as observed by *in situ* methods and how the combination of these techniques coupled with an intimate knowledge of the structure of the solids is helping to solve the remediation process. In general, the *in situ* method allows the investigator to follow the nucleation and crystal growth or phase transformations occurring in hydrothermal reactions.

1. Introduction

One of the most compelling environmental problems facing the United States is the remediation of enormous stocks of nuclear waste that exists throughout the land. The most critical waste is that accumulated as a result of our nuclear weapons program and is termed high level waste (HLW). It contains varying quantities of ^{137}Cs and ^{90}Sr and smaller amounts of actinides in the fluid part of the stored waste. This waste arose mainly as byproducts of the processes utilized for the separation of uranium and plutonium and originally stored in steel tanks underground. To prevent corrosion of the tanks the acid was treated with sodium hydroxide. This procedure precipitated the insoluble hydroxides but held in solution large quantities of alumina and silica. In most cases excess base was added so that the fluid portion existing above the solid "sludge" is 1–3 M in NaOH and 5–7 M in $NaNO_3$. Over time, evaporation has resulted in the formation of a salt cake at the top of the fluid portion.

Most of this HLW is stored at the Hanford, Washington site and in Savannah River, South Carolina with lesser amounts at Oak Ridge and the Idaho National Engineering and Environmental Laboratory (INEEL). Current thinking in terms of tank waste treatment is to remove the Cs^+ and Sr^{2+} from the fluid portion with possible dissolution of the salt cake portion for similar treatment. These elements would then be encased in a special boron glass. The remaining fluid waste could then be treated as low level waste (LLW) and made into a cement or grout that could be stored above ground. The glass containing HLW would be stored underground in steel containers [1].

Our approach to the solution of this problem is to employ inorganic ion exchangers that are highly selective for the targeted ions, mostly Sr and Cs and to a lesser extent Pu and Np. Work done at Sandia National Laboratory led to the discovery of a particular titanium silicate [2] that was highly selective for Cs^+ and to a lesser extent to Sr^{2+}. This compound was prepared as a powder by

*Author to whom all correspondence should be addressed.
0022-2461
DOI: 10.1007/s10853-006-7317-x

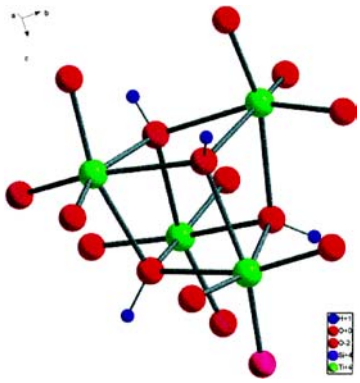

Figure 1 A portion of the titanosilicate structure in the proton form showing the cluster of four titanium-oxygen octahedra sharing edges to form the cubane-like Ti_4O_4 group. The oxygens within the cubane group are each bonded to a proton making them hydroxo-groups. The Ti atoms are yellowish green, oxygens red and hydrogens blue.

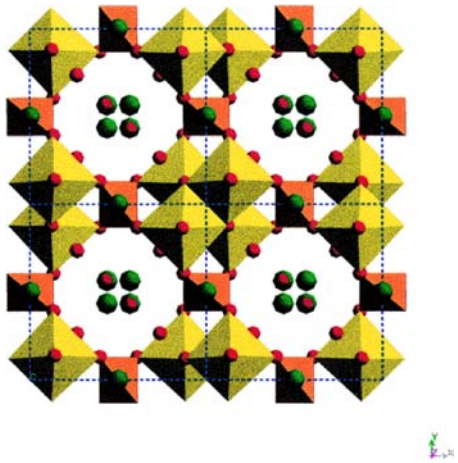

Figure 2 Top view (down the *c*-axis) of sodium titanium silicate showing the clusters of four TiO_6 octahedra (yellow) bridged by orange silicate groups with red oxygens. The tunnels are filled with Na^+ (green) and water molecules (red). The green Na^+ on top of the orange tetrahedra symbolizes the Na^+ ions sandwiched between silicate groups within the framework.

hydrothermal methods. We will refer to this phase as TS in what follows (sometimes referred to as CST). We reproduced the synthesis using titanium tetraisopropoxide $Ti(O_3C_3H_7)_4$, tetraethylorthosilicate (TEOS) and NaOH(6.32 M). We use Teflon lined pressure vessels in several sizes, 15, 30, 60, 100 and 800 ml, built in our own shops. Our first procedure used a temperature of 170°C for 8 days duration.

We were able to solve the crystal structure from the X-ray powder pattern of the hydrothermally prepared solid. The ideal composition of this compound is $Na_2Ti_2O_3(SiO_4)\cdot 2H_2O$ but the formula derived from the X-ray structure analysis was $Na_{1.64}H_{0.36}Ti_2O_3(SiO_4)\cdot 2H_2O$. The discrepancy arises from thorough washing of the powder accompanied by the hydrolysis where H^+ replaced Na^+.

The crystals are tetragonal $a = 7.8082(2)$ Å, $c = 11.9735(4)$ Å, space group $P4_2/mcm$, $Z = 4$. The titanium atoms occur in clusters of four grouped about a 4_2 axis, two up and two down rotated by 90°. Each titanium is octahedrally coordinated, sharing edges in such a way that an inner core or four oxygens and four Ti atoms form a distorted cubane-like structure (Fig. 1). These cubane-type structures are bridged to each other through silicate groups along the *a*- and *b*-axis directions. The titanium-oxygen clusters are 7.81 Å apart in both the *a*- and *b*-axis directions with the Si atoms at $Z = \frac{1}{4}, \frac{3}{4}$. In the *c*-axis direction, the Ti atoms are bridged by oxo-groups. The *c*-axis is approximately 12 Å long, which is twice the distance from the center of one cubane-like cluster to its neighbor in the *c*-axis direction. These two views of the framework are shown in Figs 2 and 3.

The net result of this framework arrangement is that tunnels are formed that are one dimensional, running along the *c*-axis direction. Perpendicular to the tunnels are vacancies in the faces or four sides of the tunnels. These cavities are just the right size to enclose sodium ions. Four silicate oxygens bond to the sodium ion at a distance of 2.414(5) Å (Fig. 3). The sodium ion coordination is completed by bonding to two water molecules in the tunnels at a bond distance of Na–O of 2.765(1) Å. Half the Na^+ ions are thus accounted for in the framework sites as there are two sodiums in each face over one *c*-axis cell length for a total of four out of the eight required per unit cell. The remaining sodiums reside within the tunnels along with the water molecules in a disordered arrangement.

The Na–O bond distances within the tunnels are longer than the sum of the ionic radii (2.42 Å [4]) at 2.76(1) Å. This bond distance measurement was made with only 64% of the sodium ion sites occupied. The deficiency of sodium arises from hydrolysis during washing so that the actual formula was $Na_{1.64}H_{0.36}Ti_2O_3(SiO_4)\ 1.8H_2O$.

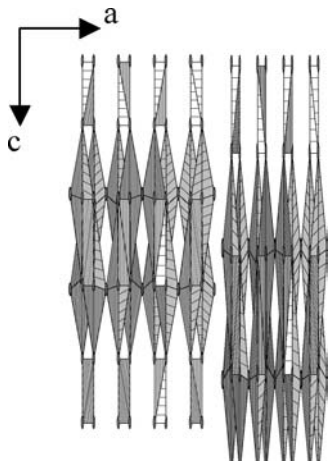

Figure 3 A polyhedral representation of the sodium titanium silicate structure showing structural features in the *c*-axis direction. The hexagonal cavities contain sodium ions which are omitted for clarity.

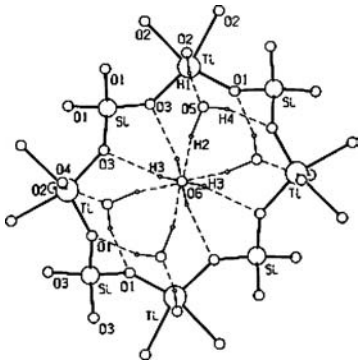

Figure 4 A ball and stick representation of a portion of the proton phase $H_2Ti_2O_3(SiO_4)_4 \cdot 1.5H_2O$ as viewed down the *c*-axis showing the hydrogen bonding scheme between the acid proton and the water molecules O5 and water–water and water-framework oxygens.

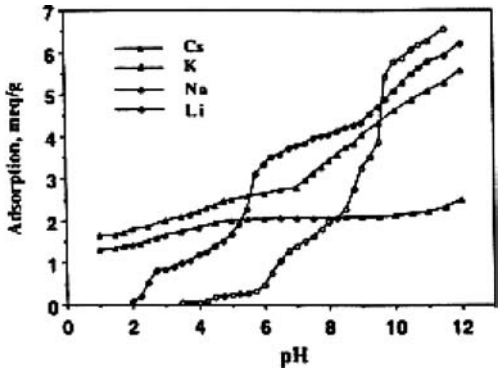

Figure 5 Potentiometric titration curves for alkali metal cations on $Ti_2(OH)_2O(SiO_4)$. $1.5H_2O$. Titrant 0.05 (MCl+MOH). Theoretical exchange capacity 8.03 meq/g.

Because of the deficiency of Na^+ the sodium ion positions were found to be disordered with partial occupancy by water (or hydronium ions). It is possible to obtain the fully occupied sodium phase by not washing the product of the hydrothermal reaction with water.

We were able to convert the sodium ion phase completely to the proton phase by exhaustive washing with 0.1 M HCl [5]. The framework remains intact but the unit cell dimensions become $a = 11.039(1)$ Å, $c = 11.886(1)$ Å, space group $P4_2/mbc$, $Z = 8$. The new *a*-axis is the diagonal of the *ab* plane of the sodium ion phase. In order to locate the protons within the structure, a neutron diffraction study was carried out [6]. The acid protons are bonded to the oxygens that form part of the cubane-like structure (Fig. 1) and are not present as hydronium ions. There are six water molecules in each tunnel per one unit cell. All the water molecule's hydrogens were located and they form a beautiful hydrogen bonded array (Fig. 4) in which all the hydrogen atoms are involved. The acid proton, H1, hydrogen bonds to a water molecule, O5, as shown in Fig. 4. The O1- - -O5 distance is 2.75(1) Å with an O1- - -H - - -O5 angle of 169(1)°. The correct formula for the proton phase is $Ti_2(OH)_2O(SiO_4)1.5H_2O$.

1.1. Structure of Cs^+ phase

Our primary interest in the sodium titanium silicate is its ability to remove cesium and strontium from nuclear waste solutions. To this end we carried out potentiometric ion exchange titrations for the alkali metals as shown in Fig. 5 [5].

Fig. 5 presents the potentiometric titration curves for alkali metals on the titanium silicate exchanger [7]. The selectivity is clearly seen in acid solution as $K^+ > Cs^+ \gg Na^+ \gg Li^+$. In fact, it turns out that the true sequence is $Cs^+ > Rb^+ \gg K^+ \gg Li^+$. However, the situation is not that simple. There are three exchange sites in this titanosilicate, the framework site, the near framework site and the center tunnel site. In order to obtain thermodynamic selectivities, it is necessary to determine to which site the ion locates so as to be able to describe the phase involved. This site determination can only be revealed by X-ray structural studies, and this study has been partially carried out in the case of Na^+, K^+ and Cs^+ [3, 5].

In the case of sodium ion, the half exchanged phase, $NaHTi_2O_3(SiO_4) \cdot 2H_2O$, was prepared by titration of the proton phase. The structure was solved, *ab initio*, using X-ray powder data. The crystals are tetragonal $a = 7.832(1)$ Å, $c = 11.945(2)$ Å, space group $P4_2/mcm$. All the sodium ions were found in the framework sites with Na–O bond distances very close to those found for the sodium ions in the framework sites in the fully exchanged phase discussed above. It is clear then, that the sodium ion prefers the framework sites exclusively, as expected.

A similar study was carried out in which Cs^+ was exchanged for H^+. We note in Fig. 5 that a significant amount of Cs^+ is exchanged in acid solution. As the pH is increased, the amount of exchange increases until about pH 6. The total exchange capacity at pH 12.0 is 1.9 meq/g or ~25% of the total milliequivalents of protons. The reason for this low level of exchange is readily apparent. The Cs^+ fits snuggly within the tunnels at Z (or c) = ¼, ¾ (Fig. 6). The Cs^+ forms 8-bonds to the silicate oxygens of 3.183(5) Å and two bonds to water of somewhat smaller size (~3 Å). Thus, the Cs–O bonds are very close to the sum of the ionic radii of Cs^+ and O^{2-}. Since the *c*-axis dimension is approximately 12 Å, the two cesium ions are 6 Å apart but the diameter of a ten coordinate Cs^+ is 3.62 Å [4]. Therefore, no additional cesium ions can fit into the tunnel. This fact accounts for the 25% capacity. The large Cs^+ cannot fit into the small framework sites nor can it occupy the near framework site at $Z = 0$, ½ when the preferred tunnel sites are occupied. However, Na^+ can fit into the framework sites and when a mixed solution of Na^+ and Cs^+ is exchanged, both types of exchange occur simultaneously [7]. The reason that more K^+ than Cs^+ is taken up in acid solutions is its smaller size. Some K^+ is able to fit into the near framework site at $Z = 0$, ½ as well as the center of the tunnel.

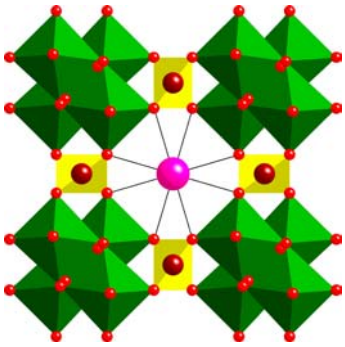

Figure 6 A polyhedral representation of the phase $NaC_{s0.5}H_{0.5}Ti_2O_3(SiO_4)\cdot H_2O$. The Cs^+ sits in the center of the tunnel at $Z = ¼, ¾$ and is 8-coordinate. The Na^+ is sited in the framework cavities at $Z = 0, ½$ (red sphere on top of yellow silicate ion).

In nuclear waste solutions it was found that the sodium titanium silicate exchanges almost no Cs^+. The apparent reason is that the very high level of Na^+ present in the waste solutions fills all the sites such that the equilibrium constant for Cs^+ in such solutions is insufficient to have Cs^+ exchange. However, it was known that substitution of 25% of the Ti sites by Nb^{5+} did allow Cs^+ to be exchanged [8]. The incorporation of this amount of Nb^{5+} was a challenge for the powder X-ray work to determine where the Nb resided. For this reason we wished to improve the crystallinity of the sodium titanium silicate and at the same time reduce the time of hydrothermal synthesis. For these purposes we undertook a more thorough *ex-situ* and *in situ* study of the hydrothermal process.

2. Experimental methods

2.1. Hydrothermal studies [9]

2.1.1. Preparation of gels

Two groups of gels were used in these studies. In the first group (group I), starting gels were prepared so that the titanium to silicon ratio (Ti/Si) was greater than 1.0, while in the second group (group II) Ti/Si = 0.5.

Preparation of group I gels. Several precursors with general composition. $1.0TiO_2{:}xSiO_2{:}yNa_2O{:}146.0H_2O$ were prepared by variation of one of the parameters and then treated hydrothermally for time τ at temperature T. The ranges of variation of x, y, T and τ were as follows: $1.01 \leq x \leq 1.6$, $3.64 \leq y \leq 5.67$, $110°C \leq T \leq 210°C$, 2 days $\leq \tau \leq$ 15 days.

Generally synthetic parameters were varied one at a time. The gels were prepared by mixing titanium isopropoxide ($Ti(OC_3H_7)_4$, 97%, Alfa Aesar) with tetraethylorthosilicate ($Si(OC_2H_5)_4$, Aldrich) in a plastic beaker. Sodium hydroxide was added to the mixture in the form of a 6.32 M solution under constant stirring, followed by addition of 15 ml of doubly deionized (ddi) water. After vigorous agitation the mixture was sealed in a 100 ml Teflon lined pressure vessel and kept in the oven. In the experiments involving variation in the composition of the gel, hydrothermal reaction was carried out for 3.5 days at 170°C.

After heating, the final products in all reactions were treated in the following fashion: pressure vessels were left at RT to cool down, the solid was separated by filtration, rinsed with ddi water and ethanol, and dried at 60°C. X-ray powder patterns of the solids were routinely recorded on a Rigaku computer-automated diffractometer with rotating anode, operated at 50 kV and 100 mA with a copper target. Data were collected from $2\theta = 5$ to 60 degrees with a step size of 0.04° and exposure time of 1 s/step.

Preparation of group II gels. A second group of precursors was prepared using a different source of silica. The general composition of these gels was $1.0TiO_2{:}1.98SiO_2{:}yNa_2O{:}218H_2O$. A total of 3.5 ml of titanium isopropoxide (Alfa Aesar) with 20 ml of ddi H_2O and 7 ml of 10 M NaOH were mixed in a plastic beaker. To this mixture, 1.469 g of silicic acid (Fisher), dissolved in NaOH solution was added. The amount of added NaOH was varied according to the desired gel compositions specified below. After agitation, the mixture was sealed in a Teflon lined pressure vessel and heated in the oven at the conditions outlined below. The X-ray powder patterns of the solids were recorded on Bruker-AXS D8 powder high resolution parallel beam X-ray diffractometer, operating at 40 kV and 40 mA. Data were collected from $2\theta = 5$ to 60 degrees with a step size of 0.04 and exposure time of 1 s/step.

2.1.2. Studies of pathways of crystallization

In the present investigation the process of crystallization was studied using *ex-situ* batch experiments as well as in-situ diffraction techniques.

Batch type ex-situ experiments. The gel of desired composition was divided into several 20 ml pressure vessels (12 ml of gel in each liner), which were sealed, and heated in an oven at a certain temperature for different periods of time. The powder pattern of each product was collected and plotted against time.

In-situ experiments. In-situ synthesis experiments were carried out at the X7B beamline of the NSLS at BNL.

A gel of composition, $1.0TiO_2{:}1.98SiO_2{:}6.77Na_2O{:}218H_2O$ was prepared by mixing of 3.5 ml of titanium isopropoxide in 20 ml of ddi H_2O, 8.5 ml of 10 M NaOH with 27 ml of 0.86 M silica solution in 2.6 M NaOH. A single crystal sapphire capillary supplied by Saphikon (0.45 mm ID and 0.75 mm OD) closed at one end with Swagelock® fitting, was filled with the gel and mounted on a goniometer head with a Swagelock® tee using a Vespel ferrule. An external nitrogen pressure of 250 psi was applied through the connected tubing and a hot air stream was used to slowly heat the capillary to 220°C at a constant rate for (2 h), and followed by a 14 h synthesis at this temperature. The hydrothermal conditions

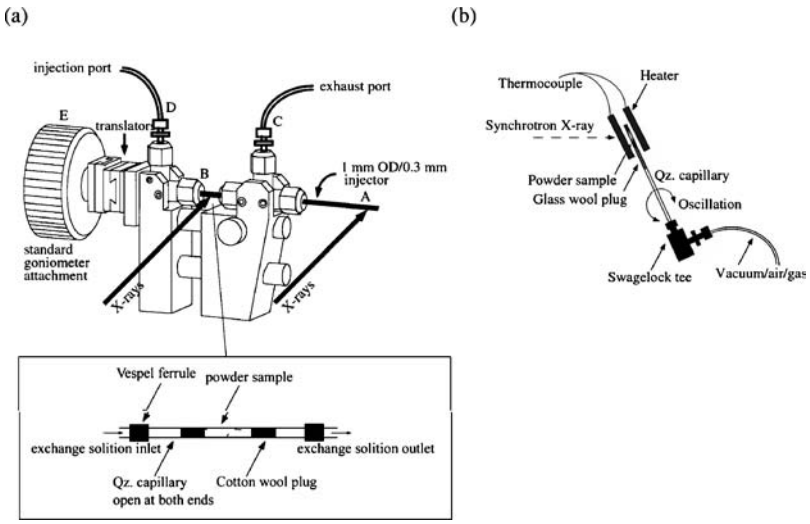

Figure 7 Apparatus used at X7B, NSLS, BNL. View of the Small Environmental Cell for Real-Time Studies (SECReTS).

were achieved in the heated part of the capillary (Fig. 7) [10,11].

Diffracted X-ray ($\lambda = 0.9223$Å) data were collected on a MAR 345 imaging plate (IP) detector with a built in scanner for online reading. Erasing, exposing and reading the IP limits the time resolution to about 2.5 min. Data were acquired for 60 s exposures. A large dynamic range can be obtained with IPs that in turn allows intensity data to be extracted from the image for Rietveld refinement of *in-situ* powder diffraction data. The wavelength, sample detector distance, zero point, and imaging plate tilt were determined using a LaB_6 standard [10, 11].

The crystallization progress was determined from IP images using integrated intensities of the diffraction lines. After data collection, IP data were integrated using the program Fit2D [12, 13]. These files were saved as a CHI file (2θ vs. intensity file), and then converted to DiffracPlus and CPI format by the program ConvX [14]. These formats were used in the programs EVA [15] (data plotting), CRYSFIRE [16] (automated indexing), XFIT [17] (peak profiling), and EXPGUI [18] (Retvield refinement) as a graphical interface for GSAS [19] for the processing of data for structure refinement.

2.1.3. Recording of the NMR spectra

Si-29 NMR spectra of several gel filtrates and filtrates from final products were recorded on a Varian Inova 400 NMR spectrometer equipped with 5 mm multinuclear probe head. Gels for NMR experiments were prepared using D_2O as a solvent. Chemical shifts were recorded with respect to $Si(CH_3)_4$ in $CDCl_3$ locked at $CDCl_3$. A 2 s acquisition time, 20 s relaxation delay, and 45° pulse was used to obtain the spectra. During the acquisition the field was locked at D_2O. A 2.620 ppm standard shift from zero was added to the chemical shifts of peaks and peak assignment was done based on corrected values.

3. Results

Hydrothermal treatment of the Group I gels consistently yielded two phases; the TS phase and a sodium titanium silicate phase of composition Na_2TiSiO_5 (STOS). This latter phase is a synthetic analogue of the naturally occurring mineral whose crystal structure was reported previously [20, 21]. The structure of STOS is built up of Ti–O square pyramids that share corners with SiO_4 tetrahedra forming layers. Sodium ions reside between the layers [22] but are not exchangeable. For gels of composition 1.0 TiO_2:1.01 SiO_2:y Na_2O:146 H_2Oy was varied from 3.6 to 5.67. The yield of STOS increased with the alkalinity of the starting gel, resulting in a pure phase for y above 5.7. The TS phase was obtained as a pure phase for y values below 3.65. However as the alkalinity decreased the crystallinity of the TS phase decreased (Fig. 8).

Open-framework compounds typically crystallize under hydrothermal conditions at temperatures up to 250°C.

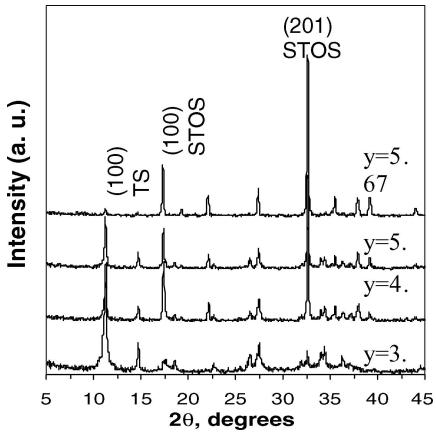

Figure 8 XRD powder patterns of solid phases obtained from Group I gel, Ti:Si = 1, $T = 170$°C, 84 h.

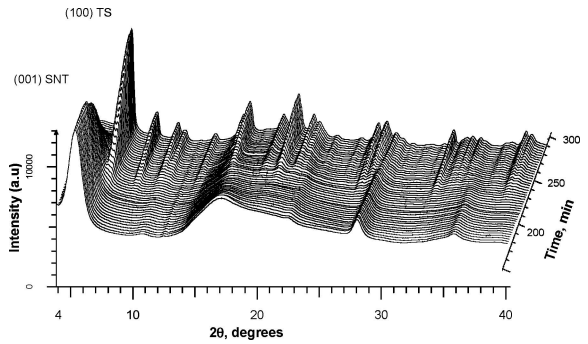

Figure 9 XRD dynamic spectra of CST crystal growth.

Too high a temperature or pressure results in formation of less open structures [23–25]. Temperatures for Group I gels were varied from 145° to 210°C. At the low temperatures a sodium titanate phase of ideal composition $Na_4Ti_9O_{20}{\cdot}nH_2O$ formed. This phase will be referred to as SNT for sodium nonatitanate [26, 27] and has been found to be highly selective for Sr^{2+} in alkaline solution [28]. Above 160°C mixtures of STOS and TS phases formed with the amount of the former increasing with temperature.

Group II Gels: *Ex-situ*: two gels were prepared in which the ratio of silica to titania was 2:1 or twice the ratio of the Group I gels. The first had a NaOH concentration of 2.7 M and the second 4.2M. The exact ratios were gel 1 1.0 TiO_2:1.98 SiO_2:6.77 Na_2O:218 H_2Ogel 2 1.0 TiO_2:1.98 SiO_2:10.53 Na_2O:218 H_2O

The temperature was 210°C. Gel 1 resulted in the formation of the TS phase of moderate crystallinity in 1 day and a highly crystalline phase in 5 days. This latter solid contained about 2% STOS. Gel 2 with a greater concentration of NaOH, yielded highly crystalline STOS both after 24 h and 5 days at *in-situ* studies. Fig. 9 shows the time resolved three dimensional plot of the X-ray patterns obtained for gel 1. The X-ray patterns were obtained every two and a half minutes with about a one minute exposure and ninety seconds for recording the pattern. We note that the first phase to appear is the sodium nonatitanate which appears as the sample was heating up to 220°C. After about 40 min the TS phase makes its appearance and continues to increase relative to the SNT phase. The entire process of transformation required 45 min until TS is the only phase present. There was no evidence for the presence of STOS for the entire eight hour run. In Fig. 10 we show the X-ray patterns prior to and during the transfer of the SNT to the TS phase. The first panel (upper left) shows the X-ray pattern of the pure SNT phase with the initial peak at $d_{001} = 9.6$Å. After 12.5 min (second panel, upper right) the first peak (100) for the TS phase is clearly evident at $d = 7.8$Å. The remaining panels show the continued growth of the TS pattern relative to that of SNT after 19.5 min and 27 min.

A similar study with gel 2, carried out *ex-situ* is shown in Fig. 11. At 200°C a poorly crystalline SNT phase is obtained that after 9 h begins to transform to the STOS phase. The TS phase does not appear as an intermediate. Similar *ex-situ* experiments at 200°C with gel 1, showed initial formation of SNT (1 h) while the TS phase began to appear after 10 h and complete conversion required about two h. A 24 h run showed the presence of pure TS phase.

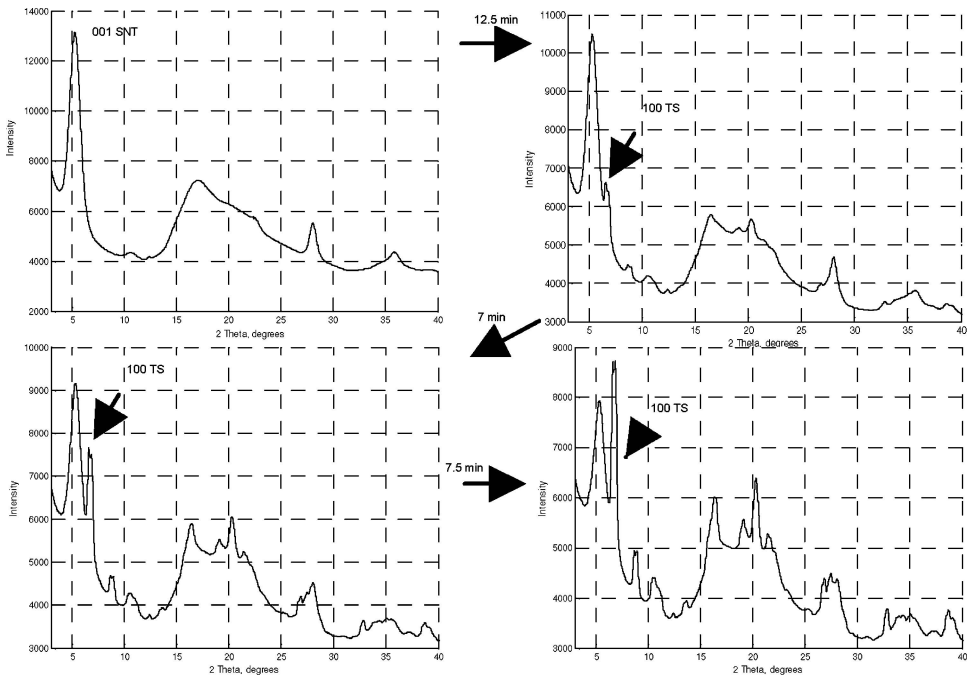

Figure 10 XRD patterns of SNT (upper right) and its transformation as a function of time to the TS phase at 220°C.

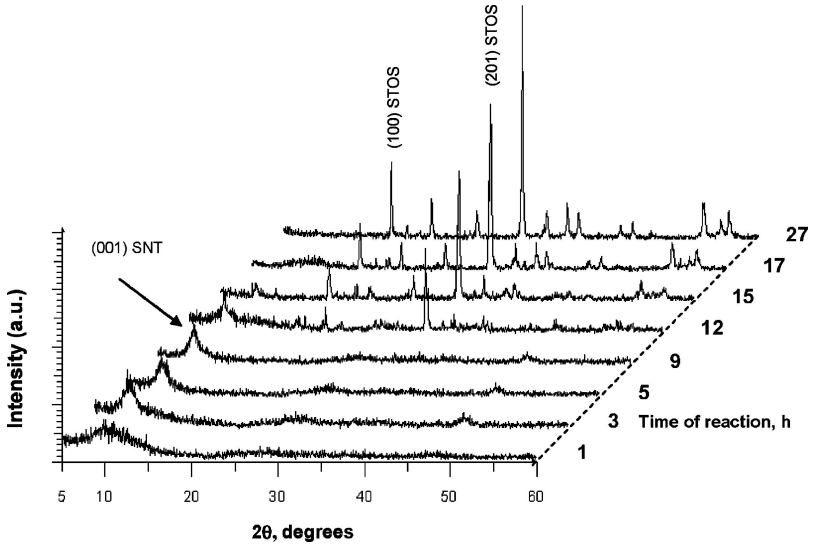

Figure 11 *Ex-situ* study of transformation of gel 2 (high NaOH content) from SNT phase to the STOS phase. No TS is evident ($T = 200^{\circ}$C).

With this information it is now possible to obtain highly crystalline TS as a pure phase.

In situ ion exchange. In our studies on Cs^+ exchange in the TS phase we indicated that the Cs^+ preferred a site in the center of the tunnel at ¼ and ¾ z. However, it was also determined that some of the Cs^+ was cited at ½ ½ 0.13 and ½ ½ 0.63 [3]. The two sites are mutually exclusive, in any one unit cell either one or the other but not both can be occupied because of the size of the Cs^+ ion. In this second site the Cs^+ is six coordinate with four bonds to framework oxygens at 3.06Å and two to water molecules at 2.95Å. These bond distances, while indicative of strong bonds, can probably not compensate for the two additional bonds in the center site in terms of free energy. That is, site 1 would be expected to create a larger ΔH exotherm than site 2. In order to shed some light on this mystery we carried out *in-situ* Cs^+ ion exchange studies at room temperature starting with the protonated phase $H_2Ti_2O_3SiO_4 \cdot 1.5H_2O$. Approximately 1 mg of H-TS was placed inside a 0.5 mm quartz capillary tube and held in place by two glass wool plugs. The capillary was mounted on the apparatus shown in Fig. 7 and hooked up to a source of 0.01 M CsCl. The sample was first wetted with water followed by the cesium chloride solution at a rate of 1 drop per 80 s. The wavelength was $\lambda = 0.9223(1)$Å and the patterns were recorded every 2.5 min (Fig. 12).

Rietveld refinement of the X-ray patterns showed that the Cs^+ initially occupied site 2. After the occupancy of site 2 reached ~18% (in 7 in) there was about 4% occupancy of site 1. Then the amount of Cs^+ in site 1 began to increase reaching a level of 22% occupancy while the site 2 stayed constant. The uptake of Cs^+ is shown by the almost immediate appearance of the (020) peak for the Cs-TS phase and the simultaneous lowering of

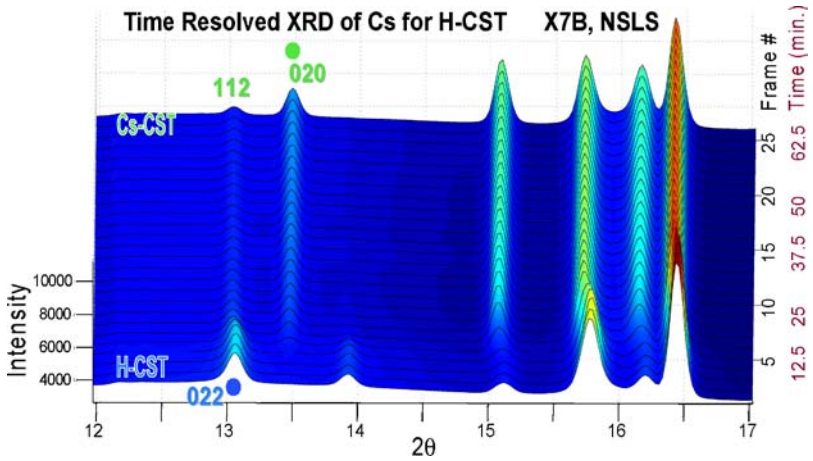

Figure 12 A zoomed 3D plot of time resolved data obtained from the X7B beam line at the NSLS. Only the first 62.5 min are shown for clarity. The sample was $H_2Ti_2O_3SiO_4o1.5H_2O$ being exchanged with Cs^+.

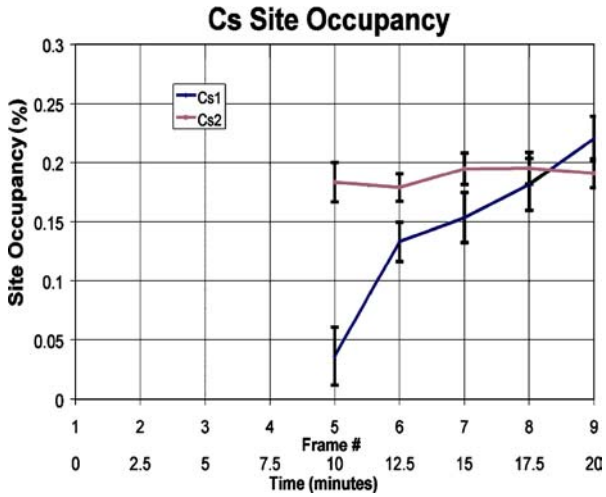

Figure 13 *in situ* resolved X-ray diffraction results showing the exchange of Cs^+ for H^+ to be a selective process with Cs 2 site filling first, followed by movement of Cs^+ into site 1.

the intensity of the H-TS peak. After about 100 min the further change was very small indicating that equilibrium is achieved rapidly (Fig. 13). The actual site uptake as a function of time is shown in Fig. 14. In about 10 min site 2 has achieved its maximum uptake and within another 10 min site 1 is loaded. How can we explain these exchange results?

The silicate silicon atoms are located at $z = \frac{1}{4}, \frac{3}{4}$ with their oxygens symmetrically displaced above and below the silicon atoms. The Cs^+ on diffusing into the tunnel encounters the four silicate oxygens at 0.17Z forming strong bonds with Cs–O equal to 3.06Å. In order to continue moving down the channel, the framework must distort to move the oxygens apart because when the Cs^+ is at 0.17 the Cs-O distance would be less than 3.0Å, smaller than an allowed bond distance. Thus, there is a barrier obstructing the motion of ions through the tunnel. As the pressure of the [Cs^+] gradient increases the Cs is forced through the barrier and now finds itself in the $Z = \frac{1}{4}$ position surrounded by eight equidistant oxygens. For the Cs^+ to further diffuse through the channel, the Cs^+ would have to move from $Z = \frac{1}{4}$ to $Z = 0.63$ where it is again 6-coordinate. These two moves, may occur in tandem reducing the energy required somewhat until the external pressure is insufficient to continue the process. At equilibrium there is still some Cs^+ in site 2.

Nb-TS It has been found that Nb-TS is able to remove sufficient Cs^+ from nuclear waste solutions to be considered for this application. We redid the structure of this phase and found that the Cs^+ is now 12-coordinate bonding to the same eight framework oxygens and four water molecules (Fig. 14) [29]. The increased coordination would increase the exothermic component of the free energy equation making the reaction thermodynamically more preferred. In addition the Cs^+ site 2 is now ten coordinate with six waters bonding to Cs^+. The increased coordination of the cesium ions arises from the fact that the Nb^{5+} increases the framework charge such that half the Na^+ in the tunnel is no longer present. Furthermore, even less sodium ion and more water is in the tunnel because of hydrolysis. Because the cesium ions retain essentially their same positions in the tunnel as for the non-Nb phase, the mechanism of exchange is likely the same in the two forms. Because of the increased coordination in both sites the selectivity is greatly increased and perhaps the barrier to diffusion somewhat lowered because of the differences in charge and water distribution.

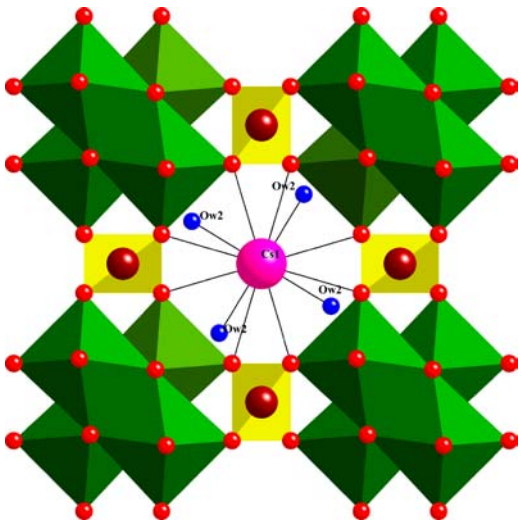

Figure 14 Polyhedral representation of $NaCs_{0.5}Nb_{0.5}Ti_{1.5}O_3SiO_4 \cdot 2.2H_2O$.

4. Conclusions

In-situ study of hydrothermal processes coupled with *ex-situ* studies has allowed us to prepare phase pure titanosilicates and uncovered the precursors and phase transformations in this sodium titanosilicate system. Initial studies including Nb in the titanosilicate gel is complicated by the presence of niobium silicate phases. Therefore companion *in-situ* hydrothermal and ion exchange studies on this system are in progress. Application to other systems such as pharmacosiderites is in the planning stages.

Acknowledgements

We acknowledge the U.S. DOE Environmental Management and Science Program, Grant DE-FG07-01ER63300 with funds supplied through the Westinghouse Savannah River Technology Center. J.P. and A.J.C. acknowledge the support of CEMS, funded through Grant NSF-CHE-0221934, and support via Grant NSF-DMR-0095633. This research was carried out in part at the National Synchrotron Light Source, Brookhaven National Laboratory, which is supported by the U.S. Department of Energy, Division of Materials Sciences and Division of Chemical

Sciences, through Contract No. DE-AC02-98CH10886. Special thanks to Dr. Jonathan Hanson, Department of Chemistry, Brookhaven National Laboratory for help at the NSLS.

References

1. W. W. SCHULZ and N. J. LOMBARDO, in " Science and Technology for Disposal of Radioactive Tank Waste," (Plenum Press, New York, 1998. Ch. 1, 2).
2. R. G. ANTHONY, R. G. DOSCH, D. GU and C. V. PHILIP, *Ind. Eng. Chem. Res.* **33** (1994) 2702.
3. D. M. POOJARY, R. A. CAHILL and A. CLEARFIELD, *Chem. Mater.* **6** (1994) 2364.
4. R. D. SHANNON, *Acta Cryst.* **A32** (1976) 751.
5. D. M. POOJARY, A. I. BORTUN, L. N. BORTUN and A. CLEARFIELD, *Inorg. Chem.* **35** (1996) 6131.
6. P. PERTIERRA, M. A. SALVADO, S. GARCIA-GRANDA, A. I. BORTUN and A. CLEARFIELD, *ibid.* **38** (1999) 2563.
7. A. I. BORTUN, L. N. BORTUN and A. CLEARFIELD, *Solv. Extr. Ion Exch.* **14** (1996) 341.
8. R. G. DOSCH, N. E. BROWN, H. P. STEPHENS and R. G. ANTHONY, Technology and Programs for Radioactive Waste Management and Environmental Restoration, Sandia National Laboratory, Albuquerque, NM, (1993), Vol. 2, p. 1751.
9. D. G. MEDVEDEV, A. TRIPATHI, A. CLEARFIELD, A. J. CELESTIAN, J. PARISE and J. HANSON, *Chem. Mater.* **16** (2004) 3659.
10. P. NORBY, *J. Am. Chem. Soc.* **119** (1997) 5215.
11. J. B. PARISE, C. L. CAHILL, Y. LEE, *The Canadian Mineralogist* **38** (2000) 777.
12. A. P. HAMMERSLEY, S. O. SVENSSON, A. THOMPSON, *Nucl. Instr. Meth.* **A346** (1994) 312.
13. A. P. HAMMERSLEY, S. O. SVENSSON, M. HANFLAND, A. N. FINCH and D. HAUSERMANN, *High Pressure Research* **14** (1996) 235.
14. M. BOWDEN, ConvX program, 1998, http://ccp14.minerals.csiro.au/ccp/web-mirrors/convx/.
15. EVA: data evaluation and plotting software, 4.0.0.2 ed. Bruker AXS: Karlsruhe, Germany, 1998.
16. R. SHIRLEY, The CRYSFIRE System for Automatic Powder Indexing: User's Manual, The Lattice Press, 41 Guildford Park Avenue, Guildford, Surrey GU2 7NL, England, 2000.
17. R. W. CHEARY, A. A. COELHO, Programs XFIT, deposited in CCP14 Powder Diffraction Library, Engineering and Physical Sciences Research Council, Daresbury Laboratory, Warrington, England, 1996, http://www.ccp14.ac.uk/tutorial/xfit-95/xfit.htm.
18. B. H. TOBY, *J. Appl. Crystallogr.* **34** (2001) 210.
19. A. C. LARSON, R. B. VON DREELE, Generalized Structure Analysis System, GSAS, Los Alamos National Laboratory: Los Alamos, NM, 1985.
20. A. V. NIKITIN, V. V. ILYUKHIN, B. N. LITVIN, O. K. MEL'NIKOV and N. V. BELOV, *Dokl. Akad. Nauk SSSR* **6** (1964) 1355.
21. Y. P. MEN'SHIKOV, Y. A. PAKHOMOVSKII, E. A. GOIKO, I. V. BUSSEN and A. N. MER'KOV, *Zap. Vses. Mineral. O-va.* **3** (1975) 314.
22. H. NYMAN, M. O'KEEFFE, *Acta Crystallogr., Sect. A* (1978) 905.
23. M. S. DADACHOV, J. ROCHA, A. FERREIRA, Z. LIN and M. W. ANDERSON, *Chem. Commun.* **24** (1997) 2371.
24. J. PLEVERT, R. SANCHEZ-SMITH, T. M. GENTZ, H. LI, T. L. GROY, O. M. YAGHI and M. O'KEEFFE, *Inorg. Chem.* **42** (2003) 5954.
25. M. NYMAN, A. TRIPATHI, J. B. PARISE, R. S. MAXWELL and T. M. NENOFF, *J. Am. Chem. Soc.* **124** (2002) 1704.
26. J. LEHTO and A. CLEARFIELD, *J. Radioanal. Nucl. Chem.* **118** (1987) 1.
27. A. CLEARFIELD and J. J. LEHTO, *Solid State Chem.* **73** (1988) 98.
28. R. A. CAHILL, Ph.D. Dissertation, Texas A&M University, College Station, TX, 1996.
29. A. TRIPATHI, D. G. MEDVEDEV, M. NYMAN and A. CLEARFIELD, *J. Solid State Chem.* **175** (2003) 72.

Received 14 May
and accepted 22 April 2005